

## Coupled effects of canal lining and multi-layered soil structure on canal seepage and soil water dynamics

Liqliang Yao<sup>a</sup>, Shaoyuan Feng<sup>a</sup>, Xiaomin Mao<sup>a,\*</sup>, Zailin Huo<sup>a</sup>, Shaozhong Kang<sup>a</sup>, D.A. Barry<sup>b,1</sup>

<sup>a</sup> Center for Agricultural Water Research in China, China Agricultural University, Beijing 100083, China

<sup>b</sup> Ecole polytechnique fédérale de Lausanne (EPFL), Faculté de l'environnement naturel, architectural et construit (ENAC), Institut d'ingénierie de l'environnement, Laboratoire de technologie écologique, Station No. 2, 1015 Lausanne, Switzerland

### ARTICLE INFO

#### Article history:

Received 17 June 2011

Received in revised form 31 December 2011

Accepted 1 February 2012

Available online 10 February 2012

This manuscript was handled by Philippe Baveye, Editor-in-Chief, with the assistance of Ram Ranjan, Associate Editor

#### Keywords:

Ponding test

Anti-seepage measures

Compacted canal bed

Numerical simulation

HYDRUS-2D

### SUMMARY

Ponding tests were conducted in the Shiyang River Basin in Northwest China to assess canal leakage characteristics. Four anti-seepage constructions (concrete lining, pebble lining, clay lining plus compacted canal bed, compacted canal bed only) were performed on four canal sections, which were situated in multi-layered soils. The canal sections were tested using a two-stage approach: First, a stable water level was maintained; second, a stage where the water level in the canal section was permitted to drop. The canal seepage rate and the soil water content near the canal bed were monitored during each stage and in each canal section. Soil texture, bulk density and hydraulic conductivity were determined in each canal section and soil layer. Double ring infiltration tests were performed to investigate infiltration behaviour from the canal sections. The saturated–unsaturated flow model HYDRUS-2D was applied to simulate canal seepage and the local soil water response. The simulation results compared well with the monitored data, indicating that the model can reliably simulate canal seepage under these complex soil structures and different canal liners. Both experimental results and numerical modelling show that the clay lining plus compacted canal bed provides the best anti-seepage performance, followed by compacted canal bed only, then pebble and concrete lining. Simulation results also predicted that the soil water content was discontinuous at the interface of distinct soil layers, and that the range and form of wetting front varied greatly in the four canal sections, with a larger wetted area for the more permeable canal. Simulations were performed to study the sensitivity of canal seepage to the permeability of each soil layer and canal liner. The results, confirmed by the double-ring infiltration tests, indicated that the canal lining is not the only factor affecting canal seepage: The soil permeability can also influence the seepage, especially where there is a low permeability layer (e.g., compacted soil layer) close to the canal.

© 2012 Elsevier B.V. All rights reserved.

### 1. Introduction

Canal seepage is the main water loss during agricultural water conveyance (Wang et al., 2002). Besides the loss of water resources, it causes the groundwater table to rise and can produce soil salinization in areas with high evaporation (Change et al., 1985; Salama et al., 1999). On the other hand, canal seepage can help maintain groundwater levels and support plant growth or water supplies in rural areas (Meijer et al., 2006). It is thus beneficial to understand the process of canal seepage, factors that influence it and the fate of infiltration water (e.g., the induced soil water

dynamics around the canal, deep percolation, and amount of groundwater recharge).

Canal seepage is usually estimated by seepage meters, ponding tests and inflow–outflow tests (Brockway and Worstell, 1968; Alam and Bhutta, 2004). Rantz (1982) introduced the inflow–outflow method to monitor canal seepage rates in detail. However, the ponding method is considered the most accurate and dependable method for measuring canal seepage (Brockway and Worstell, 1968; Kraatz, 1977). For example, both ponding and inflow–outflow tests were used to evaluate the seepage losses in the Fordwah Eastern Sadiqia (South) irrigation system, with the conclusion that the ponding method is more accurate (Alam and Bhutta, 2004).

The main factors influencing canal seepage are the canal linings, the soil hydraulic properties and their spatial variations, the canal cross-sectional profile and water level, the groundwater table location, and the amount of sediment inside the canal (Kraatz, 1977).

The influence of the canal lining was investigated experimentally by Wilkinson (1986), Moghazi (1997), Meijer (2000) and

\* Corresponding author. Tel./fax: +86 10 6273 6533.

E-mail addresses: [liqliang85327@gmail.com](mailto:liqliang85327@gmail.com) (L. Yao), [fsy@cau.edu.cn](mailto:fsy@cau.edu.cn) (S. Feng), [maoxiaomin@tsinghua.org.cn](mailto:maoxiaomin@tsinghua.org.cn) (X. Mao), [huozl@163.com](mailto:huozl@163.com) (Z. Huo), [kangshaozhong@tom.com](mailto:kangshaozhong@tom.com) (S. Kang), [andrew.barry@epfl.ch](mailto:andrew.barry@epfl.ch) (D.A. Barry).

<sup>1</sup> Tel.: +41 21 693 5576; fax: +41 21 693 8035.

Meijer et al. (2006). It was found that a suitable canal lining can reduce the seepage rate considerably. However, in some circumstances, a high-cost lining might not decrease canal leakage greatly and a low-cost lining could have a better cost/benefit performance. For example, even without extra canal lining, canals located on compacted soil beds can compete well with the lined canals, resulting in lower overall costs (Moghazi, 1997).

Soil hydraulic properties and soil structure below the canal can also influence canal seepage. Measurements have shown that seepage rates are influenced by the condition and composition of canal banks, and to a lesser extent by soil texture (Kahlown and Kemper, 2004). Most canals are located in areas with complex multi-layered soil conditions. Experiments indicate that the infiltration into layered soils can differ markedly from those in homogenous soils (Fok, 1970; Hillel and Parlange, 1972; Wang et al., 1999). If the anti-seepage lining is considered as one layer of the multi-layered porous medium, then canal seepage can be regarded as an infiltration process into a multi-layered soil composed of a distinct weakly permeable lining layer, and a series of natural soil layers. The combined effect of these layers on canal seepage has seldom been studied experimentally (Rastogi and Prasad, 1992; Moghazi, 1997; Islam, 1998).

Based on field experiments, empirical formulas have been established to estimate canal seepage for various situations (ICID, 1967; Krishnamurthy and Rao, 1969; Cui et al., 2004). Although such formulas are convenient for practical applications, they involve considerable simplification and cannot show the seepage development spatially and temporally.

Theoretical analyses of canal seepage have been reported also. Harr (1962) and Morel-Seytoux (1964) have given some analytical solutions for seepage from canals in a deep, homogeneous isotropic porous medium. Bouwer (1965, 1969) and Mirnateghi and Bruch (1983) presented solutions for seepage problems related to irrigation canals, concluding that the canal seepage increased linearly with increasing elevation of the canal bed during the steady seepage stage, and that the water table depth decreased linearly with increasing canal bed elevation. Ram et al. (1994) proposed an analytical solution for the problem of water table rise owing to the combined action of canal recharge and surface infiltration. More recently, Choudhary and Chahar (2007) obtained an exact analytical solution for the quantity of recharge/seepage from an array of rectangular canals underlain by a drainage layer at a finite depth and with pressure. Analytical solutions improve predictions compared with empirical formulas in that they permit calculation of the canal seepage loss and show the seepage development spatially and temporally. However, because of simplifications needed for analytical tractability, they cannot show variations of canal seepage with different canal sections, soil characteristics and groundwater levels.

Numerical simulation provides a means to understand more thoroughly the process involved in canal seepage. Wachyan and Ushton (1987) modified the solutions of Bouwer (1969) using a numerical method. Soneneshein (2001) and Luo et al. (2003) calculated canal seepage with a MODFLOW groundwater model. These numerical models concentrated either on the groundwater response, assuming the canal seepage as the source to the groundwater surface, or on the infiltration process in the unsaturated zone. However, canal seepage leads to saturated–unsaturated soil water movement (including possibly perched water) in the vadose zone. This is especially the case for lined canals, which are designed to have lower saturated hydraulic conductivity ( $K_s$ ) than the surrounding soil, thereby leading to positive (i.e., greater than atmospheric) pressure water infiltration in the upper area and unsaturated (less than atmospheric pressure) flow in the lower area. Dages et al. (2008) verified one such model based on field experiments, and evaluated groundwater recharge from seepage

losses in a ditch. Rastogi and Prasad (1992) simulated canal water infiltration in the canal-phreatic aquifer system assuming the conductivity of the lined material was one-tenth that of the topsoil. Phogat et al. (2009) simulated the process of canal seepage and groundwater table response under different canal bed elevations using HYDRUS-2D (Šimůnek et al., 2008). They analysed a laboratory experiment, and demonstrated that increasing the canal bed elevation leads to linearly increasing canal seepage and linearly decreasing groundwater table depth.

Besides the aforementioned studies of canal seepage, there is little detailed work on seepage processes examining the coupled effects of the canal lining and the soil layering, although they are common phenomena in the field and affect both soil water dynamics and groundwater recharge. To investigate the effects of these characteristics of real canals, ponding tests were carried out on canal sections with various liners and multi-layered soil conditions in the Shiyang River Basin (Northwest China). This is a farming region dependent on canal diversions and irrigation, and is affected by water shortages. Clearly, a validated numerical model would provide support for optimising canal anti-seepage treatments as part of strategies for efficient utilisation of water resources in this and other arid regions. Based on the ponding test results and supplementary experiments, the HYDRUS-2D numerical model was applied to simulate the canal seepage and induced soil water response. These efforts aimed to identify and quantify the main factors influencing canal seepage, as well as to understand soil water dynamics occurring due to canal seepage.

## 2. Material and methods

### 2.1. Experimental design and measurements

#### 2.1.1. Study area

Field experiments were carried out at the Shiyanghe Experimental Station for Water-Saving in Agriculture and Ecology, located in Northwest China, on the border of the Tenger Desert (N37°52'20", E102°50'50", altitude 1581 m above sea level). The site is in a typical continental temperate climate zone with a mean annual temperature of 8 °C. The mean annual precipitation is 164 mm and pan evaporation is 2000 mm. Average annual sunshine duration is 3000 h with over 150 frost-free days. The groundwater table is 40–50 m below the ground surface.

#### 2.1.2. Ponding test

A canal of 120 m long with a trapezoidal cross-section was constructed in the Shiyanghe Experimental station (Fig. 1) following the Chinese technical standard (Ministry of Water Resources of China, 2005). The canal was partitioned into four sections using concrete plates. The sections were equipped with concrete lining (shortened as CL), pebble lining (PL), clay lining plus compacted canal bed (CC) or compacted canal bed only (CO). Experiments were performed over the period 25 June–15 August 2008.

Ponding tests were conducted in each canal section. These tests comprised two stages, with the first stage approximating a constant water level (by water addition) and the second allowing the free water level to drop (no water added). The second test was not conducted for the CC section because the clay liner cracked after the first test. A water gauge was installed in each section to control and monitor the canal water level in the first stage, and in the second stage for calculating the canal seepage rate. To monitor the response of the soil water around the canal, four vertical Trime pipes were installed in the middle of each canal section. The soil water content variations in vertical soil layers were measured using a Time Domain Reflectometry (TDR) Trime-tube system (Laurent et al., 2001, 2005) at 10-cm intervals and 2.8 m

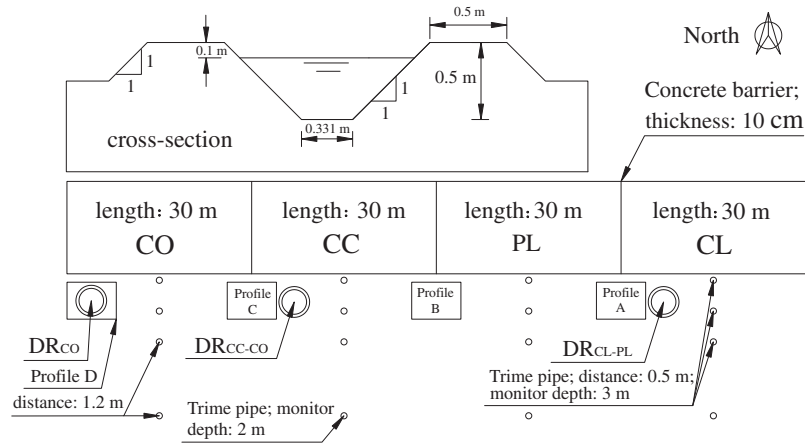


**Fig. 1.** Sketch of the experimental design and associated measurements for: concrete lined canal (CL), pebble lined (PL), clay lined plus compacted canal bed (CC) and compacted canal bed only (CO); 12 Trime pipes; soil profiles A, B, C and D; double-ring tests  $DR_{CL-PL}$ ,  $DR_{CC-CO}$  and  $DR_{CO}$ .

depths in each pipe. Fig. 1 depicts the experimental design and associated measurements for canal sections of CL, PL, CC and CO.

### 2.1.3. Canal bed soil texture measurements

Profiles A, B, C and D in Fig. 1 were excavated to depths of 3 m, 2.8 m, 1.5 m and 1.5 m, respectively. Two soil samples were taken at 20-cm intervals in each pit; these were used to determine particle size distributions using laser diffraction (Eshel et al., 2004). According to the soil texture and colour, the profiles were divided into 5 (profile A), 6 (B), 5 (C) and 4 (D) layers. Two soil samples were taken in each layer to measure  $K_s$  using a constant-head permeameter (Klute, 1986), and the dry bulk density determined by the oven drying, using a cutting ring with a sample size of  $100 \text{ cm}^3$  (Lai and Ren, 2007).

### 2.1.4. Double-ring infiltration tests

Three double-ring infiltration tests were conducted near profiles A (denoted in Fig. 1 as  $DR_{CL-PL}$ ) and C ( $DR_{CC-CO}$ ), and at profile D ( $DR_{CO}$ , this profile was excavated following the double-ring infiltration test). A double-ring test was also planned near profile B, but this experiment failed because of an operational error. The diameter of inner ring was 80 cm, and the diameter of outer ring was 100 cm. The water level in the inner ring was maintained using a Mariotte tube, while the water level in the outer ring was adjusted manually to match that in the inner ring. The Mariotte tube was 180 cm high, with a 20-cm inner diameter. It was graduated from 0 to 170 cm in 0.1-cm subdivisions, allowing visual readings. Lai and Ren (2007) provide details of the experimental procedure.

### 2.1.5. Meteorology measurements

An automatic weather station monitored precipitation, air temperature, air humidity, wind speed, etc. Pan evaporation was measured hourly by an E601 evaporation pan (Fu et al., 2009) in the weather station.

## 2.2. Model description

### 2.2.1. Mathematical basis

Due to the longitudinal extent of the canal sections, it was assumed that the canal seepage and resulting soil water movement around the canal in the ponding test can be simplified to two dimensions (2D). The governing model for water flow is Richards equation (Šimůnek et al., 2008):

$$\frac{\partial \theta}{\partial t} = \frac{\partial}{\partial x} \left[ K(h) \frac{\partial h}{\partial x} \right] + \frac{\partial}{\partial z} \left[ K(h) \left( \frac{\partial h}{\partial z} + 1 \right) \right], \quad (1)$$

where  $x$  is the horizontal coordinate [L],  $z$  (positive upward) is the vertical coordinate [L],  $t$  is time [T],  $\theta$  is the volumetric water content [ $\text{L}^3 \text{L}^{-3}$ ],  $h$  is the pressure head [L] (soil water matric potential in the unsaturated zone) and  $K(h)$  is the soil hydraulic conductivity [ $\text{L T}^{-1}$ ]. For the saturated zone,  $\theta$  is the saturated water content and does not vary temporally. It is different from the normal groundwater model where confined water storage is considered (e.g., Bear, 1972; Barry et al., 2007).

For unsaturated flow, several models are available to describe the relationship between  $\theta$  and  $h$ , e.g., the BC model (Brooks and Corey, 1966), the VG model (van Genuchten, 1980), and the modified VG model (Vogel and Cislserova, 1988). Here, the van Genuchten–Mualem (VGM) model, which is a combination of VG model for soil water retention curve and hydraulic conductivity function of Mualem (1976), was used:

$$\theta(h) = \begin{cases} \theta_r + \frac{\theta_s - \theta_r}{(1 + |\alpha h|)^m}, & h < 0, \\ \theta_s, & h \geq 0, \end{cases} \quad (2)$$

$$K(h) = K_s S_e^l \left[ 1 - (1 - S_e^{1/m})^m \right]^2, \quad (3)$$

$$S_e = \frac{\theta - \theta_r}{\theta_s - \theta_r}, \quad (4)$$

where  $S_e$  is the normalised water content,  $\theta_r$  and  $\theta_s$  denote the residual and saturated water contents, respectively,  $\alpha$  is the inverse of the air-entry value (or bubbling pressure),  $n$  is a pore-size distribution index,  $m = 1 - 1/n$ , and  $l$  is a pore-connectivity parameter. The parameters  $\alpha$ ,  $n$  and  $l$  are soil-specific coefficients.

Numerical solutions to the model described by Eqs. (1)–(4) were obtained using HYDRUS-2D (Šimůnek et al., 2008), a program capable of simulating 2D saturated–unsaturated water flow problems based on Galerkin finite element method. HYDRUS-2D can handle various boundary conditions (e.g., constant head, variable head, constant flux, atmospheric boundary, etc.). To calculate the cumulative infiltration as required in this research, the procedure was as follows: (1) for each time step all pressure heads were obtained by solving the governing model, and then the flux was calculated using Darcy's Law and the nodal head values; (2) the flux along the infiltration boundary (canal bed) was summed up to give the infiltration rate. Multiplying this rate by the time step and summing gives the cumulative infiltration. Note that this procedure was done automatically within HYDRUS-2D.

### 2.2.2. Model setup

Because the canal is relatively small and the test duration is relatively short, the research area was set to be 20 m horizontally (perpendicular to the canal) and 10 m vertically. We assume the flow was symmetric around the vertical axis through the middle of the canal. To save time only half of the research domain was simulated. The domain was discretized using an irregular triangular mesh, the density of which was greatest near the trapezoidal section since in that region the soil water content varies rapidly.

Vertical boundaries at each end of the simulated area (denoted  $S_1$ ) were set as zero flux boundaries. The ground surface boundary ( $S_2$ ) was also taken as a zero flux boundary. This condition ignored evapotranspiration since this is small compared with the canal water seepage rate. The canal surface ( $S_3$ ) was taken as a constant water head boundary during the first stage of the ponding test (note that the pressure head along the canal surface varied with elevation, and even became negative for zones above the water surface). The bottom boundary ( $S_4$ ) was set to be a free drainage boundary because the groundwater level in study area is relatively low.

For the first stage (fixed canal water level), the conditions on  $S_1$ ,  $S_2$ ,  $S_3$  and  $S_4$  are:

$$\frac{\partial(h+z)}{\partial \mathbf{N}} = 0, \quad (x, z) \in S_1 \cup S_2, \quad 0 \leq t \leq t_m, \quad (5)$$

$$h + d = h_w, \quad (x, z) \in S_3, \quad 0 \leq t \leq t_m, \quad (6)$$

$$\frac{\partial h}{\partial z} = 0, \quad (x, z) \in S_4, \quad 0 \leq t \leq t_m, \quad (7)$$

where  $\mathbf{N}$  is the normal direction to the boundary,  $d$  is the vertical distance to the bottom of canal,  $h_w$  is the water level in canal (40 cm in this test), and  $t_m$  is the duration of the first (stable) stage of the ponding test.

## 3. Experimental results and analysis

### 3.1. Precipitation and evaporation from water surface

One rainfall event occurred during the experiment, on 25 June 2008. The precipitation and evaporation from water surface data were quantified using water balance. Evaporation rates as a percentage of seepage rates were, respectively, 2.08, 2.24, 19.44 and 12.68 for the canal sections CL, PL, CC and CO.

### 3.2. Soil characteristics

#### 3.2.1. $K_s$

Table 1 shows the  $K_s$  values (two samples) in the four soil profiles. The results indicate marked spatial heterogeneity between the profiles in the horizontal direction. Within the profiles, most variability was evident in profiles A and C. For each profile, the maximum  $K_s$  was located at 80 cm below the ground surface. Moreover, for the same elevations, most of the measured data in profiles C and D were smaller than the corresponding data in profiles A and B.

#### 3.2.2. Soil texture

Table 1 shows the soil texture for the four soil profiles. The classification was based on soil texture triangle of the United States Department of Agriculture (e.g., Hillel, 1998). The main soil texture for all profiles was silt loam, although there was a higher proportion of sand in profiles A and B and a higher proportion of silt in profiles C and D. The maximum sand content in profiles A, C and D was found at 60–80 cm, where  $K_s$  is also a maximum. This indicates that  $K_s$  is influenced greatly by the sand content.

Because the ground surface near canal sections CO and CC was compacted before the test, the dry soil density in this area tends to be larger than for sections PL and CL, especially near the ground surface. For example, the maximum dry bulk density of the surface soil (0–20 cm) was found in profile C ( $1.99 \text{ g cm}^{-3}$ ), while the minimum dry bulk density was found in profile A ( $1.67 \text{ g cm}^{-3}$ ).

### 3.3. Ponding test results

#### 3.3.1. Cumulative infiltration during the stable water level stage

Fig. 2 shows the relationship between cumulative infiltration and time during the stable water level stage. The canal seepage rate was relatively large during the initial phase of the test, and gradually decreased with time until it stabilised. This is a common phenomenon for infiltration (e.g., Philip, 1969; Barry et al., 1995b), especially into a dry soil. It is caused by the increasing dominance of gravity-driven flow over capillarity-driven flow with increased penetration depth of the infiltrating water (e.g., Barry et al., 1993).

For the four canal sections, the cumulative infiltration in CL and PL (Fig. 2a and b) were similar and larger than the other two sections. CC showed the smallest cumulative infiltration, i.e., overall the clay-lined canal (CC) had a smaller infiltration rate than CO (Fig. 2c and d), which did not have a lining. Although canal lining is important for infiltration, the characteristics of the soil under the canal bed should also influence it, e.g., the compacted canals (CC and CO) even showed lower cumulative infiltration than the uncompact canals (CL and PL). From the soil texture measurements (Table 1), the silt content near the canal bed (0–100 cm below ground) of CL and PL are far less than that in the canal beds of CC and CO, while the sand content showed the opposite trend. Moreover, the measured  $K_s$  values (Table 1) for profiles C (near the canal bed of CC) and D (near the canal bed of CO) are much less than the corresponding values for profile A (near the canal bed of CL and PL). This demonstrates that the soil characteristics near the canal bed dominates the canal seepage, and results in the cumulative infiltration of CC and CO being far less than that of CL and PL. This agrees with previous research, e.g., based on measurements from old channels and reconstructed channels with moderately compacted banks. Kahlown and Kemper (2004) concluded that the soil characteristics (i.e., soil density, soil texture) are the main factors influencing the infiltration capacity of an earth canal, especially soil bulk density, while Moghazi (1997) concluded that, by compacting the channel bed, the rate of seepage is reduced considerably. Soil compaction is considered a cheap and an alternative method to minimise the rate of water losses in field canals (Kraatz, 1977; Burt et al., 2010).

Fig. 2 shows that the infiltration tests, carried out sequentially, gave different results, with consistently greater infiltration in the first test. The time interval between the tests was 1–2 months, so for the second test the soil profile was partially saturated initially. This confirms that the initial moisture content in the soil profile is an important factor influencing infiltration from canals and that a dry soil has a larger infiltration capacity (e.g., Parlange et al., 1999).

#### 3.3.2. Infiltration during the falling water level stage

Fig. 3 shows the variations of water levels in the canal sections during the falling water level stage. The water levels in the first test drop faster than the corresponding levels in the second, again because of the higher initial moisture content of the latter. The water level drops linearly with time (correlation coefficient above 0.99) for the duration of the experiments. Obviously, with longer times the infiltration rate should drop gradually, partly because the water level is dropping and partly because the hydraulic gradient is decreasing (e.g., Barry et al., 1995a). However, the canal section has a trapezoid shape, with smaller size at bottom, such that the

**Table 1**  
Soil profile division into distinct zones based on soil texture, and related soil hydraulic properties for each canal section.

Canal section name	Layer number	Soil depth (cm)	Soil particle size distribution (%)			Soil texture	Soil bulk density (g cm <sup>-3</sup> )	$\theta_r$ (cm <sup>3</sup> cm <sup>-3</sup> )	$\theta_s$ (cm <sup>3</sup> cm <sup>-3</sup> )	$\alpha$ (cm <sup>-1</sup> )	$n$	Measured $K_s^c$ (cm min <sup>-1</sup> )		Estimated $K_s$ (cm min <sup>-1</sup> )	Calibrated $K_s$ (cm min <sup>-1</sup> )
			Sand (>0.05 mm)	Silt (0.05–0.002 mm)	Clay (<0.002 mm)							$K_{s1}$	$K_{s2}$		
CL	Lining layer 1	6 cm-thick concrete	– <sup>a</sup>	–	–	–	–	0.067	0.45	0.02	1.41	<sup>d</sup>	–	0.0098	
		0–20	38.821	57.902	3.277	Silt loam	1.67	0.022	0.252	0.0612	1.6328	0.00341	0.00254	0.01356	0.0038
		20–48	60.652	37.412	1.936	Sandy loam	1.71	0.0257	0.3039	0.0278	1.4224	0.01195	0.01380	0.01885	0.0129
		48–86	86.139	13.259	0.602	Sand	1.56	0.04	0.3616	0.0426	2.3736	Failed <sup>b</sup>	0.13089	0.16321	0.131
		86–126	37.303	59.356	3.341	Silt loam	1.64	0.0292	0.3108	0.0174	1.4143	0.00246	0.01383	0.01534	0.0081
5	126–1000	21.605	74.482	3.913	Silt loam	1.56	0.0387	0.3522	0.0085	1.5709	0.02798	0.01496	0.02163	0.0215	
PL	Lining layer 1	6 cm-thick pebble	–	–	–	–	–	0.067	0.45	0.02	1.41	<sup>d</sup>	–	0.0096	
		0–30	30.318	66.808	2.875	Silt loam	1.56	0.0331	0.3329	0.0054	1.6867	0.00046	0.000657	0.02270	0.0038
		30–70	32.364	65.09	2.547	Silt loam	1.43	0.0348	0.3531	0.0052	1.6977	0.00577	0.00660	0.03796	0.0098
		70–92	20.159	76.104	3.737	Silt loam	1.42	0.0432	0.3832	0.0063	1.6482	0.02334	0.01123	0.03738	0.0173
		92–112	18.276	77.44	4.285	Silt loam	1.48	0.0431	0.3752	0.007	1.6218	0.00814	0.00271	0.02831	0.0054
		112–164	62.087	36.361	1.553	Sandy loam	1.52	0.0277	0.3425	0.0392	1.4184	0.0112	Failed	0.03856	0.0112
6	164–1000	57.704	40.11	2.186	Sandy loam	1.54	0.0276	0.3362	0.0333	1.3998	0.00115	0.00027	0.03110	0.0007	
CC	Lining layer 1	10 cm-thick clay	–	–	–	–	–	0.07	0.36	0.005	1.09	<sup>d</sup>	–	0.0006	
		0–30	22.535	73.335	4.131	Silt loam	1.99	0.0271	0.2737	0.0297	1.3424	0.00112	0.00014	0.00368	0.00031
		30–60	26.265	70.249	3.486	Silt loam	1.48	0.0379	0.3568	0.0076	1.5957	Failed	0.00592	0.03060	0.00121
		60–90	40.98	56.821	2.199	Silt loam	1.39	0.031	0.3441	0.0115	1.5071	0.05895	Failed	0.04119	0.00059
		90–120	12.351	82.799	4.85	Silt	1.47	0.0476	0.3942	0.0068	1.6306	0.02249	0.01311	0.02705	0.0178
5	120–1000	8.061	87.776	4.163	Silt	1.48	0.0493	0.4082	0.0072	1.6264	0.00262	0.01280	0.02505	0.00771	
CO	1	0–30	27.014	68.998	3.989	Silt loam	1.57	0.0357	0.3378	0.031	1.346	0.00275	0.00454	0.02051	0.00365
		30–60	18.508	76.69	4.802	Silt loam	1.49	0.044	0.3769	0.032	1.4283	0.00042	0.00023	0.02615	0.00036
		60–90	34.793	62.169	3.038	Silt loam	1.47	0.0328	0.3377	0.0104	1.5229	0.00940	0.00746	0.03033	0.00843
		90–1000	10.599	83.37	6.031	Silt	1.49	0.0504	0.4015	0.0066	1.6351	0.00047	0.00142	0.02245	0.000705

<sup>a</sup> “–” Means no measurement.

<sup>b</sup> “Failed” means we planned this test, but this experiment failed because of operational errors.

<sup>c</sup> “Measured  $K_s$ ” shows the data measured in soil profiles A, B, C and D, which represent the simulation areas of CL, PL, CC and CO respectively.

<sup>d</sup> These  $K_s$  values were calibrated, while the corresponding hydraulic parameters ( $\theta_r$ ,  $\theta_s$ ,  $\alpha$ ,  $n$ ) were assumed equivalent to soils with similar permeabilities.

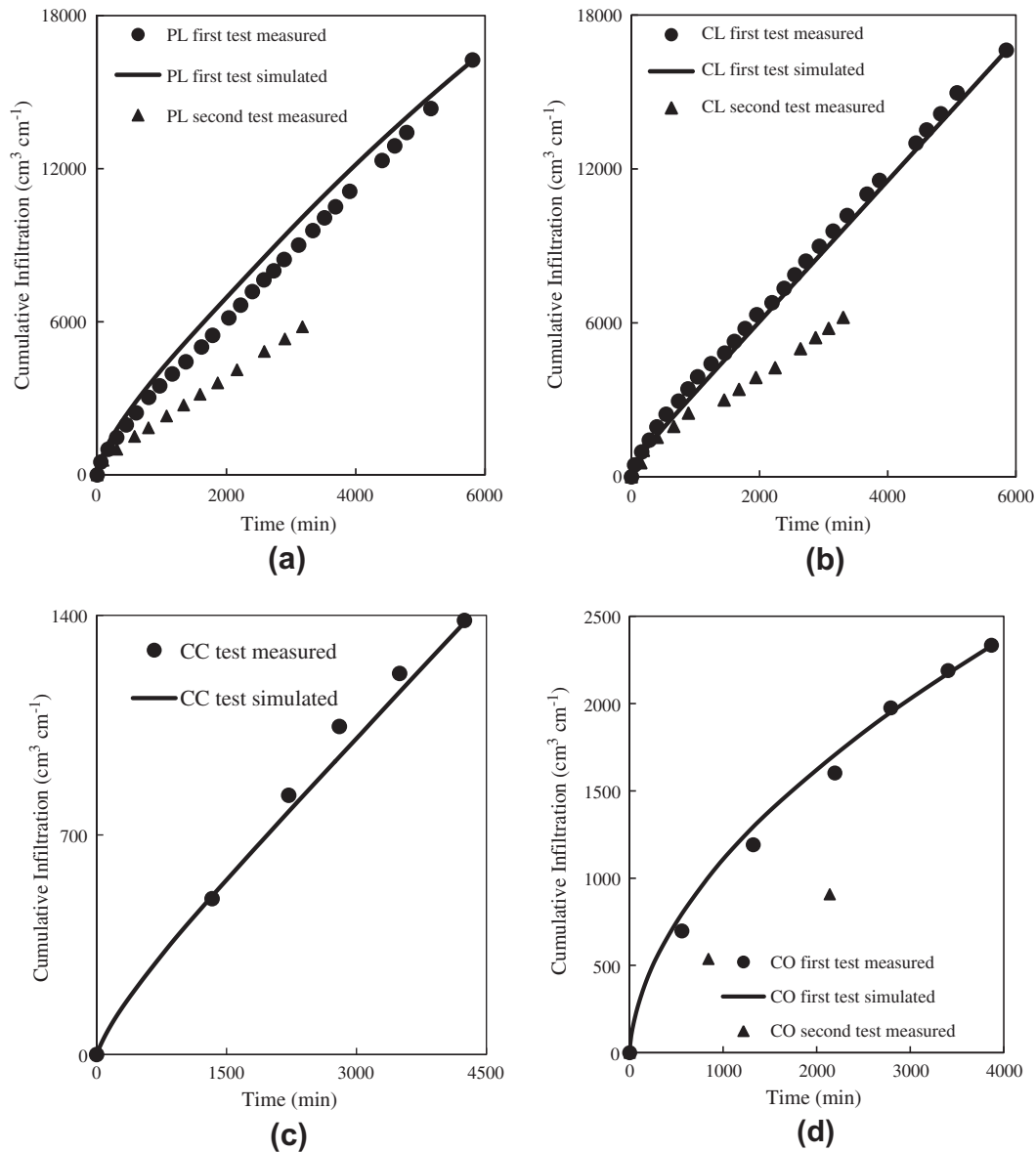


Fig. 2. Comparison of simulated and measured cumulative infiltration per unit length of canal, for the canal sections: (a) CL; (b) PL; (c) CC and (d) CO.

coupled effect of the decreasing infiltration rate and the decreasing water surface area leads to the linear drop of canal water level.

### 3.3.3. Soil water dynamics

To show soil water response to canal seepage, we show colour-coded contours of the change in water content constructed from the measured data (Figs. 4 and 5). Note that, for layered soil, normally the soil water potential is continuous but water content can be macroscopically discontinuous in the interface. Therefore, filled contours with data interpolation cannot fully represent this layered property. However, we drew the contour on the basis that TDR measurements were taken at 10-cm intervals vertically, which almost fully represents this discontinuous property in layered soil.

Fig. 4a–c shows the variation of soil water content in CL after about 2, 3 and 6 d of seepage, calculated by subtracting the measured soil water content on June 24 from that on June 26, 27 and 30 in 2008, respectively. Fig. 5 shows the variation of soil water content in CO after about 6 d of seepage, i.e., the difference of measured data between July 10 and July 16, 2008. These figures show that, due to soil layering, the soil water content does not increase uniformly.

For CL, the water infiltrated quickly into the soil, with a more rapid motion vertically than horizontally. The wetting front reached 1.2 m below the ground surface after 2 d, 1.8 m after 3 d and 2.8 m after 6 d of seepage. In the horizontal direction, the wetting front in most layers was 1.3–1.8 m from the canal midpoint and it reached over 1.8 m in some layers after 6 d of seepage. However, for CO, the water infiltrated relatively slowly into the soil. After 6 d of seepage, there is no distinct increase of soil water content under the canal bed, with the only noticeable water increase occurring within 1.7 m of the middle of the canal in the horizontal direction. These results are in accordance with the measured cumulative infiltration, which shows that there was a lower amount of infiltration into CO compared with CL.

### 3.4. Influence of soil compaction on infiltration – double-ring tests along the canal

The aforementioned data demonstrates that the infiltration is influenced by both canal lining conditions and the hydraulic characteristics of the soil layers under the canal bed, particularly if there are compacted soil layers. To identify further the influence

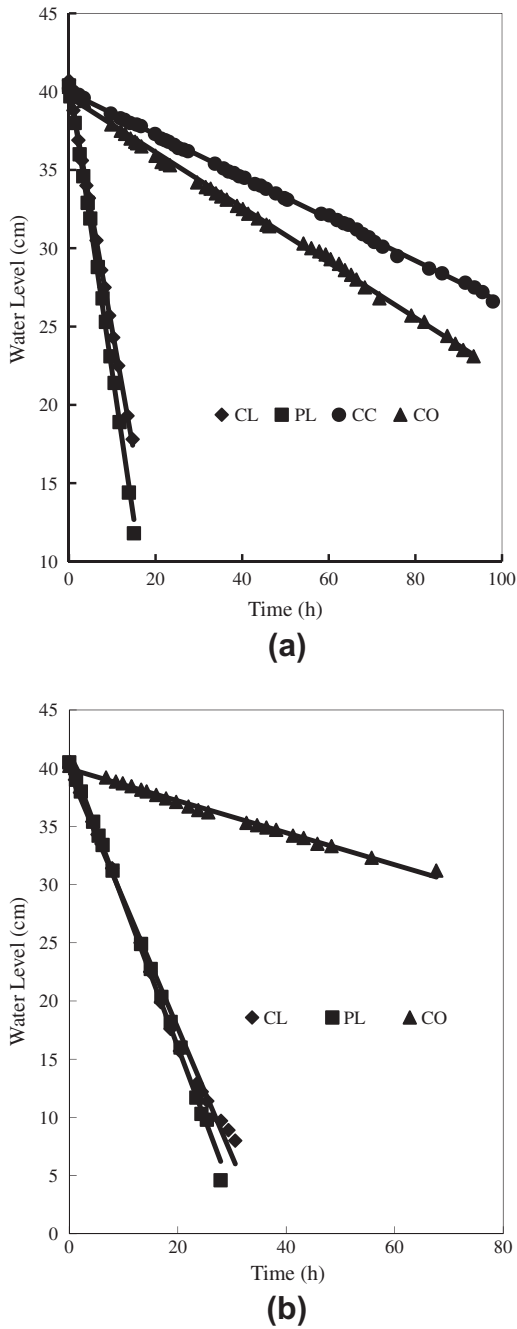


Fig. 3. Variation of water head in CL, PL, CC and CO during the falling water level stage: (a) for the first ponding test; (b) for the second ponding test.

of the multi-layered soil structures, three double-ring infiltration tests were conducted along the canal (Fig. 1). These were aimed at characterising the infiltration without the effect of the anti-seepage liners. Double-ring test DR<sub>CL-PL</sub> between CL and PL represents uncompacted soil layers, while test DR<sub>CC-CO</sub> between CO and CC and test DR<sub>CO</sub> at one end of CO both represent compacted soil layers.

Fig. 6 shows the cumulative infiltration for the three double-ring tests. The slopes of the curves are relatively high initially and decrease gradually, suggesting a steady infiltration rate. The initial higher infiltration in curve DR<sub>CO</sub> is caused by the fact that the surface soil in profile D was ploughed. With time, however, curve DR<sub>CL-PL</sub> shows the highest cumulative infiltration, followed by curve DR<sub>CC-CO</sub> and curve DR<sub>CO</sub>. These results confirm the

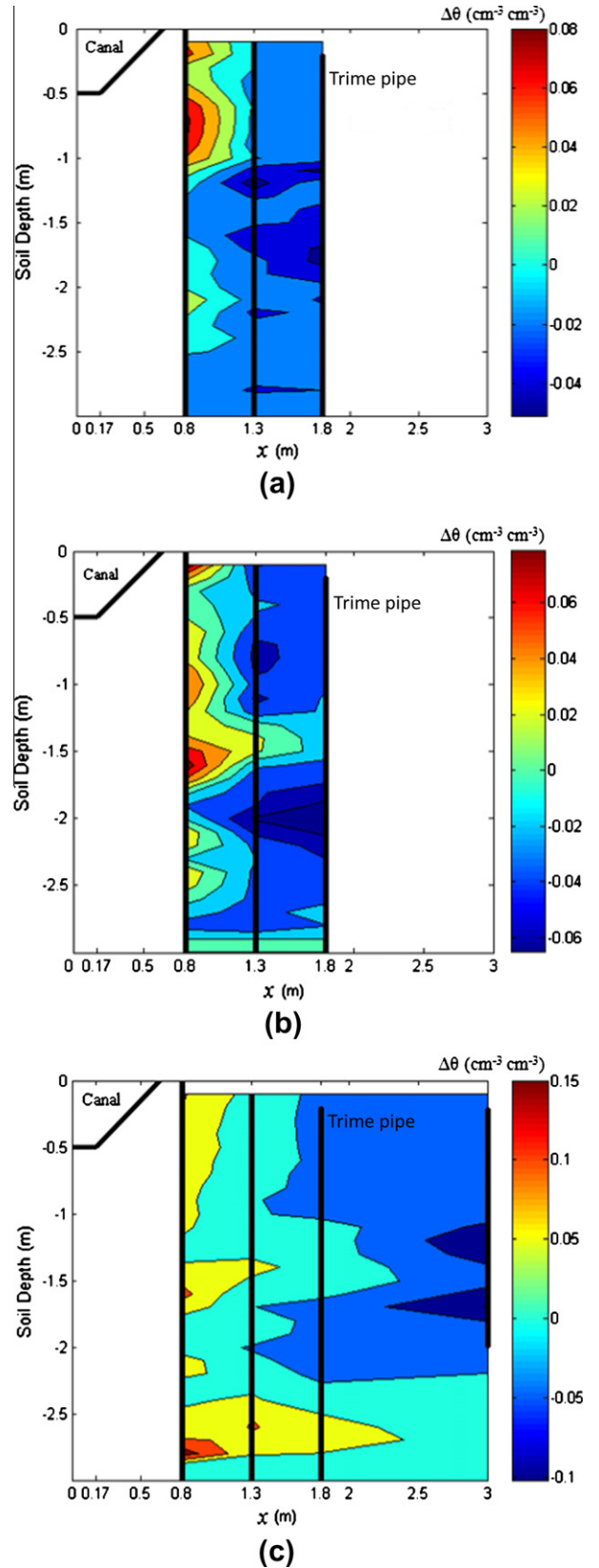


Fig. 4. Change in soil water content ( $\Delta\theta$ ) in CL for the first ponding test: (a) after about 2 d of seepage; (b) after 3 d of seepage; (c) after 6 d of seepage.

significant role played by the compacted soil layers in reducing infiltration (Moghazi, 1997). Burt et al. (2010) also concluded that canal seepage can be reduced considerably with moderately

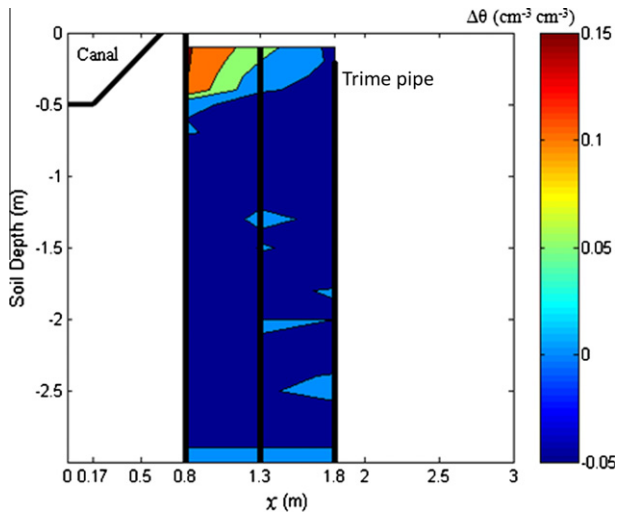


Fig. 5. Change in soil water content ( $\Delta\theta$ ) in CO after about 6 d of seepage for the first ponding test.

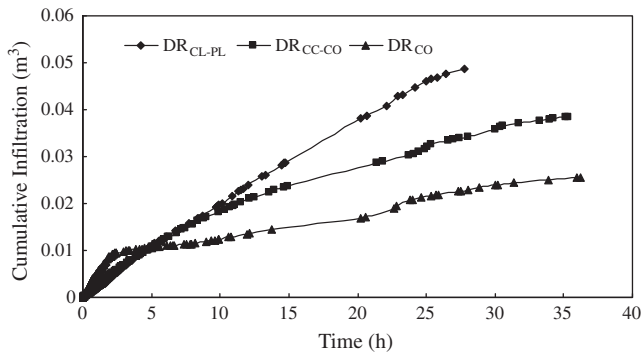


Fig. 6. Cumulative infiltration for the three double-ring tests conducted along the canal.

compacted sides and bottoms of the earthen canals. To some extent, the anti-seepage effect of the compacted canal bed may exceed the effect of anti-seepage lining, which explains why PL and CL (with pebble or concrete lining on the uncompacted canal bed) show larger cumulative infiltration than CO (without lining, but located on compacted canal bed).

### 3.5. Data preparation for modelling based on experiment results

According to the measured soil texture and  $K_s$ , the experimental site displays significant spatial heterogeneity. We assumed that the measured data near each canal section as representative of that simulation area (i.e., the measured data from the soil profiles at A, B, C and D represent the simulation areas of CL, PL, CC and CO, respectively).

Each canal section was simulated separately. The zone division considers the measured data on soil texture, hydraulic conductivity and dry bulk density. Because the canal lining was also a porous medium, it was modelled using Richards' equation and the VGM model, and was treated as a distinct zone within HYDRUS-2D. Note that (1) hydraulic characteristic parameters for this layer were unknown and had to be assumed; and (2) because the simulation area was larger than the measured area and there was no measured data in the deeper area, the lowermost measurements were used to characterise deeper, unsampled areas. The possible error caused by this assumption is discussed below.

Based on the measured soil texture and the measured  $K_s$ , the simulation areas of CL, PL, CC and CO were divided into 5, 6, 5 and 4 layers, respectively, in addition to the lining layer. Using the measured soil texture and the dry bulk density, the soil moisture characteristic parameters were obtained with the Artificial Neural Network method within the Rosetta program, which is embedded in HYDRUS-2D (Schaap et al., 2001). Note that although Rosetta also estimated  $K_s$  for each soil, these values were calibrated according to the measured infiltration rate. According to Shi et al. (2006), the  $K_s$  values for concrete and pebble liners are in the ranges of 0.00417–0.01181  $\text{cm min}^{-1}$  and 0.00625–0.01736  $\text{cm min}^{-1}$ , respectively. The calibration is within this range. For the other hydraulic function parameters, we adopted values for soils that had a similar value of  $K_s$ . The value of  $K_s$  for the silt loam is close to that of the liners (0.0075  $\text{cm min}^{-1}$ ). Thus, the hydraulic parameters ( $\theta_r$ ,  $\theta_s$ ,  $\alpha$ ,  $n$ ) of silt loam were chosen to represent these two liners (concrete and pebble). Likewise, for the clay liner, the calibration showed its  $K_s$  is close to that of the silty clay, so the latter's parameters ( $\theta_r$ ,  $\theta_s$ ,  $\alpha$ ,  $n$ ) were chosen to represent this layer. A sensitivity analysis showed that  $K_s$  is the main factor influencing seepage rate and the soil water content, providing the lining layer is thin. The value of  $l$  was set equal to 0.5 (Mualem, 1976). The layer divisions and the related soil moisture characteristic parameters for each canal section were listed in Table 1.

Soil water content was monitored by the TDR Trime-tube system in the four vertical Trime pipes in each canal section, before the start of the ponding test. They were used as the initial moisture content in the simulations. Note that, in the modelling of infiltration with perched water, HYDRUS-2D requires the pressure head as the initial condition, so the monitored soil water contents were transformed to the soil water matric potential based on values in Table 1 and the VGM model. This led to discontinuities in matric potential across the soil layers, so the potential was adjusted to achieve continuity along the profile. Based on this, the first stage, with a relatively stable canal water level was simulated for the different anti-seepage treatments.

## 4. Simulation results and discussion

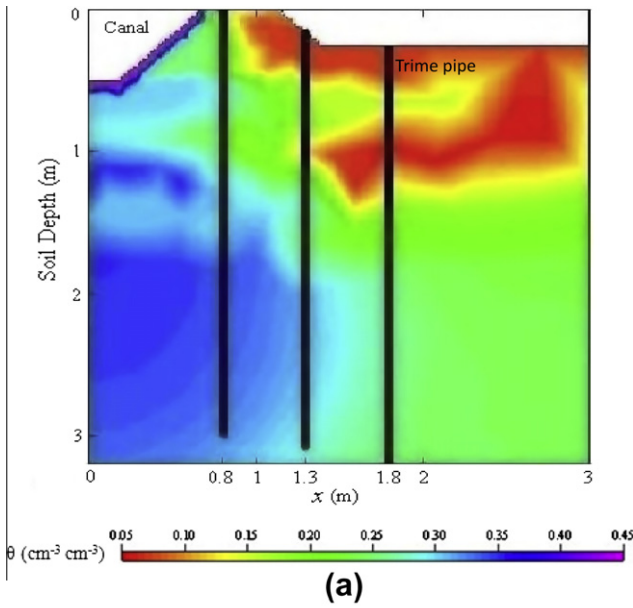
### 4.1. Cumulative infiltration

Fig. 2 shows the comparison of simulated and measured cumulative infiltration per unit length of canal, for the canal sections CL, PL, CC and CO, respectively, for the fixed head condition in the canal. Generally, the simulated results agree well with the measured data. The differences between measurements and simulations could be due to the poorly resolved soil characteristics and uncertainty in the initial soil water condition. Both the simulation and measured data show infiltration into the CL and PL sections considerably exceeds that into the CC and CO sections. For CL and PL, after the initial transient, the cumulative infiltration increases linearly with time. However, for CC and CO, the cumulative infiltration increases nonlinearly throughout the test.

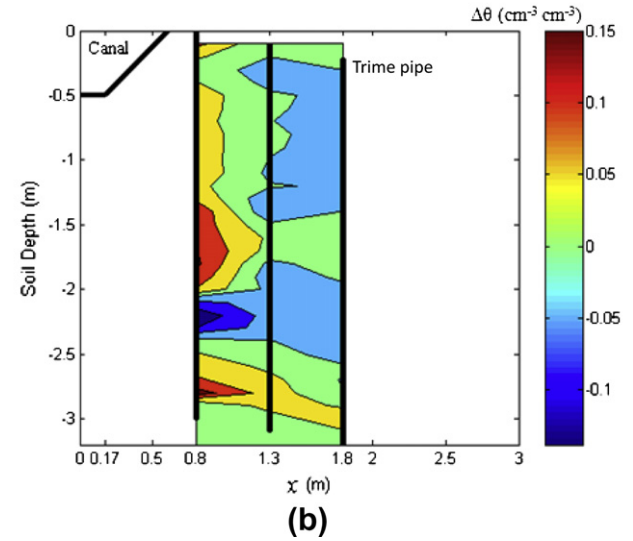
### 4.2. Soil water dynamics near the canal bed

Figs. 7a and 8a show the simulated soil water content for canal sections CL and CO at the end of the simulation, i.e., after 5851 min (about 4 d) and 3868 min (about 2.5 d) of canal seepage, respectively. For comparison, the variations of measured soil water content, i.e., the measured data at about 4 d and 2.5 d after the test began minus the measured data before the test started, are shown in Figs. 7b and 8b, respectively.

Fig. 7a shows that in CL the simulated wetting front located at over 3 m below the ground surface. Water moved about 1.5 m



(a)



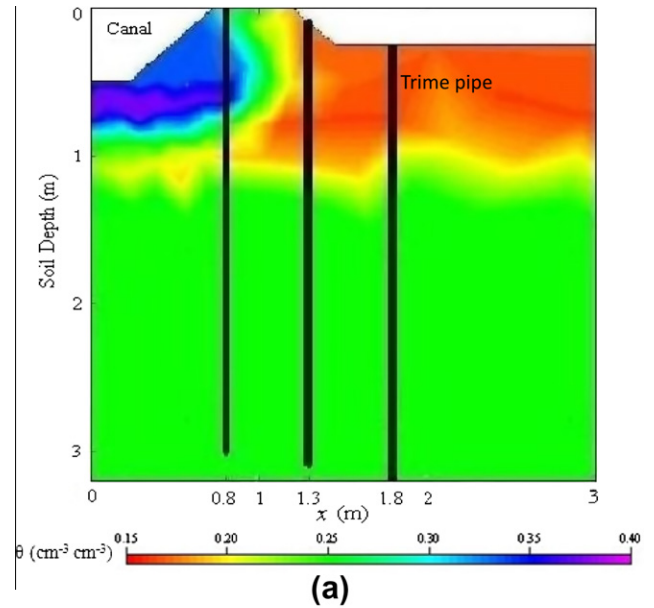
(b)

**Fig. 7.** Evolution of soil moisture for canal section CL at the end of stable water level stage: (a) simulated soil water content; (b) change in measured soil water content.

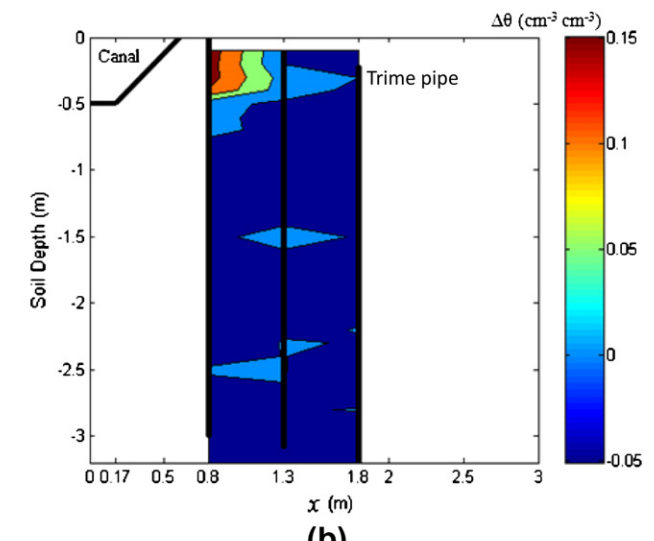
horizontally from the canal middle. The measured data (Fig. 7b) shows the wetted area reached over 2.8 m vertically and 1.8 m horizontally after about 4 d of infiltration, which is reasonably consistent with the simulation. Moreover, the measured and simulated results all show some characteristics of layering, with higher water content increases for dense soil zones. There are two layers having a marked water increase (more clearly shown in the measured data). This comparison shows a degree of similarity between the simulations and measured data.

For canal section CO, Fig. 8a shows the simulated wetting front reached about 0.7 m vertically, and about 1.1 m horizontally from the canal middle. These features compare well with the measured data in Fig. 8b, which shows the wetted area reaching about 0.7 m vertically and 1.3–1.8 m horizontally.

Both the simulations and measured data suggest that the infiltrating water penetrated the canal section CO much less than in section CL. This is consistent with the measured and simulated results for cumulative infiltration, reported above. The results also indicate that the simulations reflect reasonably well the soil water



(a)



(b)

**Fig. 8.** Evolution of soil moisture for canal section CO at the end of the stable water level stage: (a) simulated soil water content ( $\theta$ ); (b) change in measured soil water content ( $\Delta\theta$ ).

content variation due to canal seepage under the complex soil conditions present below the canal.

#### 4.3. Sensitivity of permeability of each layer on canal seepage

To study the impact of the permeability of canal lining and the layered soil on canal seepage, sensitivity simulations were performed by varying  $K_s$  of the lining layer and the soil layers. Fig. 9 shows the relative variation of the cumulative infiltration with the variation of  $K_s$  (expressed as the ratio to the original value) in each layer, for canal sections CL, PL, CC and CO respectively. Most results in Fig. 9 suggest that the seepage increases with the increase of hydraulic conductivity, and vice versa. However, the extent of the increase varied for each canal section and for each layer.

For the lining canal with most infiltration (i.e., PL and CL, Fig. 9a and b), soil layer 2 is the most sensitive layer, followed by the liner layer and soil layer 1. This occurs because soil layer 2 is adjacent to the canal bottom and the liner layer is too thin (only 0.06 m) to

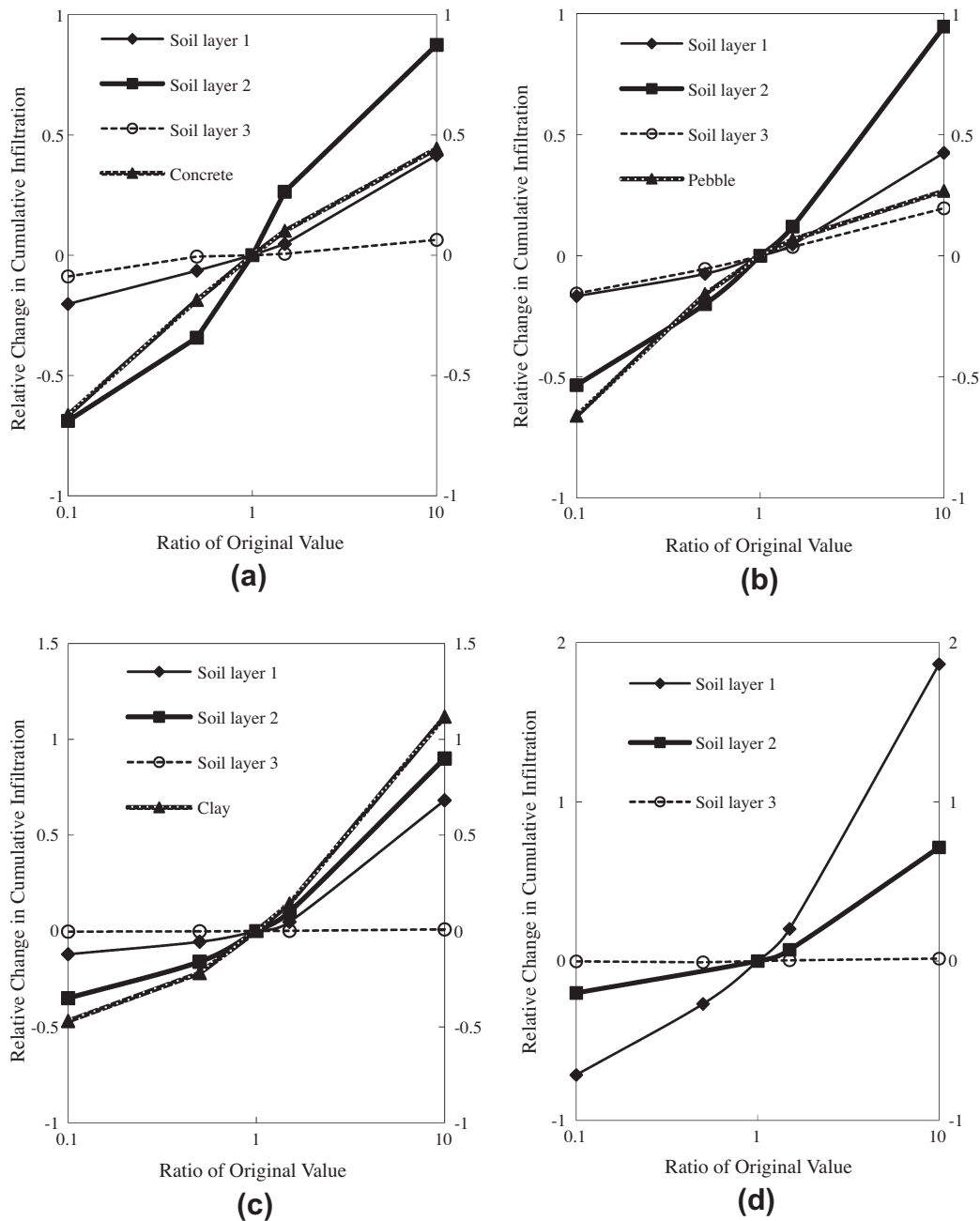


Fig. 9. Variation of cumulative infiltration with the changed  $K_s$  in each layer, for canal sections: (a) CL; (b) PL; (c) CC and (d) CO.

dominate the infiltration. Therefore, the seepage is most sensitive to the permeability of soil layer under the canal bed, followed by the liner layer.

For the lining canal with lower seepage (i.e., CC, Fig. 9c), the most sensitive layer is the clay liner layer, followed by soil layer 2 and soil layer 1. This is because the clay liner layer is thicker (0.1 m), and because the original  $K_s$  of clay liner layer is very low. Because the rate of wetting front movement tends to be greater in the vertical direction than in the horizontal direction, the infiltration is most sensitive to the permeability of the liner layer, followed by the layer under the canal bed, i.e., soil layer 2.

For the canal with less infiltration and no liner (i.e., CO, Fig. 9d), soil layer 1 is obviously the most sensitive layer, followed by soil layer 2. This is different from the canal section CC, because in this case the rate of wetting front advancement in the horizontal direc-

tion is greater than in the vertical direction. Therefore, the infiltration is most sensitive to the upper soil layer, which is around the canal.

Fig. 9a–d all shows that the canal seepage is not sensitive to the variation in  $K_s$  in soil layer 3 even though layer 3 in PL and CL are highly permeable (see Table 1). As for CC and CO, there is almost no influence on canal seepage due to the variation of  $K_s$  in soil layer 3, whether the original value of  $K_s$  is large (in CO) or small (in CC). We conclude that the seepage rate is most sensitive to the permeability variation of the surrounding layers, and so water losses can be reduced considerably with moderately compacted banks or compacted soil cores in canal banks (Kahlowan and Kemper, 2004). However, the seepage rate is insensitive to more distant soil layers, especially when the seepage rate is low. It also indicates that the simulated canal seepage would not be greatly influenced if differ-

ent assumptions were made about the soil texture or hydraulic conductivity further from the canal.

#### 4.4. Effect of the liner on seepage

To study further the impact of canal lining on canal seepage, simulations were performed by removing the concrete lining layer for CL (named CL<sub>rc</sub>) and adding the concrete lining layer for CO (named CO<sub>ac</sub>).

The seepage without the liner (CL<sub>rc</sub>) did not increase noticeably compared with that for CL; the increase was less than 6%, indicating the concrete liner is not the only factor influencing canal seepage in this region.

The seepage from CO decreased more than 16% shortly after adding the concrete liner to the canal (CO<sub>ac</sub>). Although both have a canal liner, the cumulative seepage for CL is much larger than for CO<sub>ac</sub>, indicating again that the soil under the liner layer plays an important role in controlling the canal seepage.

### 5. Conclusions and perspectives

Liners are often used to reduce canal leakage. Ponding tests were conducted in the Shiyang River Basin in Northwest China to quantify canal seepage and soil water movement as influenced by different anti-seepage liners and multi-layered soils. This study investigated four liner types, and included the effect of soil layering at the experimental site. Numerical simulations based on HYDRUS-2D were shown to compare well with the monitored data. Further simulations quantified the effect of the canal liner and soil layering structure on canal seepage. The combination of canal lining and a low-permeability layer below the canal is effective in reducing canal seepage. In consequence, compaction of the canal bed before canal lining is recommended. Also, the selection of the lining itself should be based on an analysis of local conditions such as the permeability of the soil under the canal bed, construction materials, and maintenance requirements.

The validated model is site-specific and local scale. Indeed, the numerical simulations were not intended to capture large-scale canal seepage. Such a step would involve characterisation of site heterogeneity, as well as suitable field experiments on canal leakage. In this context, the present model provides an excellent basis for experimental design and analysis. More specifically, we anticipate building on our findings to develop more quantitative tools (e.g., canal leakage prediction or design of monitoring networks) for canal losses considering spatially variable layered soil properties.

#### Acknowledgement

The research was sponsored by the National Natural Science Foundation of China (Grant Nos. 91125017, 50979105, 50909094).

#### References

Alam, M.M., Bhutta, M.N., 2004. Comparative evaluation of canal seepage investigation techniques. *Agric. Water Manage.* 66, 65–76.

Barry, D.A., Parlange, J.-Y., Sander, G.C., Sivaplan, M., 1993. A class of exact solutions for Richards' equation. *J. Hydrol.* 142, 29–46.

Barry, D.A., Parlange, J.-Y., Haverkamp, R., 1995a. Comment on "Falling head ponded infiltration" by J.R. Philip. *Water Resour. Res.* 31, 787–789.

Barry, D.A., Parlange, J.-Y., Haverkamp, R., Ross, P.J., 1995b. Infiltration under ponded conditions: 4. An explicit predictive infiltration formula. *Soil Sci.* 160, 8–17.

Barry, D.A., Lockington, D.A., Jeng, D.-S., Parlange, J.-Y., Li, L., Stagnitti, F., 2007. Analytical approximations for flow in compressible, saturated, one-dimensional porous media. *Adv. Water Resour.* 30, 927–936.

Bear, J., 1972. *Dynamics of Fluids in Porous Media*. American Elsevier, New York.

Bouwer, H., 1965. Theoretical aspects of seepage from open channels. *J. Hydraul. Div., Am. Soc. Civil Eng.* 91, 37–59.

Bouwer, H., 1969. Theory of seepage from open channel. *Adv. Hydrosci.* 5, 121–172.

Brockway, C.E., Worstell, R.V., 1968. Field evaluation of seepage measurements methods. In: *Proceedings of the Second Seepage Symposium*, ARS 41–147, USDA, Agricultural Research Service, Phoenix, Arizona, pp. 121–127.

Brooks, R.H., Corey, A.T., 1966. Properties of porous media affecting fluid flow. *J. Irrigat. Drain. Div., ASCE* 72(1R2), 61–88.

Burt, C.M., Orvis, S., Alexander, N., 2010. Canal seepage reduction by soil compaction. *J. Irrigat. Drain. Div., ASCE* 136, 479–485.

Change, C., Kozub, G.C., Mackay, D.C., 1985. Soil salinity status and its relation to some of the soil and land properties of three irrigation districts in southern Alberta. *Can. J. Soil Sci.* 65, 187–193.

Choudhary, M., Chahar, B.R., 2007. Recharge/seepage from an array of rectangular channels. *J. Hydrol.* 343, 71–79.

Cui, Y.L., Li, Y.H., Mao, Z., Lance, J.M., Musy, A., 2004. Strategies for improving the water supply system in HCID, upper reaches of the Yellow River Basin, China. *Agric. Eng. Int., CIGR J. Sci. Res. Develop.* 6 (Manuscript LW 02 005).

Dages, C., Voltz, M., Ackerer, P., 2008. Parameterization and evaluation of a three-dimensional modelling approach to water table recharge from seepage losses in a ditch. *J. Hydrol.* 348, 350–362.

Eshel, G., Levy, G.J., Mingelgrin, U., Singer, M.J., 2004. Critical evaluation of the use of laser diffraction for particle-size distribution analysis. *Soil Sci. Soc. Am. J.* 68, 736–743.

Fok, Y.-S., 1970. One-dimensional infiltration into layered soils. *J. Irrigat. Drain. Div., ASCE* 96, 121–129.

Fu, G.B., Stephen, P., Charles, Yu J.J., 2009. A critical overview of pan evaporation trends over the last 50 years. *Clim. Change* 97, 193–214.

Harr, M.E., 1962. *Groundwater and Seepage*. McGraw-Hill, New York.

Hillel, D., 1998. *Environmental Soil Physics*. Academic Press, New York.

Hillel, D.E., Parlange, J.-Y., 1972. Wetting front instability in layered soils. *Soil Sci. Soc. Am. Proc.* 36, 697–702.

ICID, 1967. *Controlling Seepage Losses from Irrigation Canal: Worldwide Survey*, New Delhi, India.

Islam, M.Z., 1998. Seepage losses in irrigation canals: a case study in Bangladesh. *Int. Agric. Eng. J.* 7, 123–146.

Kahlown, M.A., Kemper, W.D., 2004. Seepage losses as affected by condition and composition of channel banks. *Agric. Water Manage.* 65, 145–153.

Klute, A., 1986. Water retention: laboratory methods. In: Klute, A. (Ed.), *Methods of Soil Analysis. Part 1. Agronomy Monograph No. 9, second ed.* ASA and SSSA, Madison, WI.

Kraatz, D.B., 1977. *Irrigation Canal Lining. Land and Water Development Series No. 1*. FAO, Rome, Italy.

Krishnamurthy, K., Rao, S.M., 1969. Theory and experiment in canal seepage estimation using radioisotopes. *J. Hydrol.* 9, 277–293.

Lai, J.B., Ren, L., 2007. Assessing the size dependency of measured hydraulic conductivity using double-ring infiltrometers and numerical simulation. *Soil Sci. Soc. Am. J.* 71, 1667–1675.

Laurent, J.-P., Ruelle, P., Delage, L., Bréda, N., Chanzy, A., Chevallier, C., 2001. On the use of the TDR Trime-tube system for profiling water content in soil. In: *Proceedings TDR'01, Evanston-Illinois, USA, 5–2 September 2001*, pp. 1–10.

Laurent, J.-P., Ruelle, P., Delage, L., Zairi, A., Ben Nouna, B., Adjmi, T., 2005. Monitoring soil water content profiles with a commercial TDR system: comparative field tests and laboratory calibration. *Vadose Zone J.* 4, 1030–1036.

Luo, Y.F., Khan, S., Cui, Y.L., Beddek, R., Baozhong, Y., 2003. Understanding transient-losses from irrigation supply systems in the Yellow River Basin using a surface groundwater interaction model. In: *Proceedings of MODSIM 2003-International Congress on Modeling and Simulation, Townsville, Queensland, Australia*, pp. 242–247.

Meijer, K.S., 2000. *Impacts of Concrete Lining of Irrigation Canals*, Uda Walawe, Sri Lanka. M.Sc. Thesis, University of Twente, The Netherlands.

Meijer, K., Boelee, E., Augustijn, D., van der Molen, I., 2006. Impacts of concrete lining of irrigation canals on availability of water for domestic use in southern Sri Lanka. *Agric. Water Manage.* 83, 243–251.

Ministry of Water Resources of China, 2005. *Standard for Engineering Technique of Seepage Prevention on Canal*. China Water Resources and Hydropower Press, Beijing, China.

Mirnatoghi, A., Bruch, J.C., 1983. Seepage from canals having variable shape and partial lining. *J. Hydrol.* 64, 239–265.

Moghazi, H.E.M., 1997. A study of losses from field channels under arid region conditions. *Irrigat. Sci.* 17, 105–110.

Morel-Seytoux, H.J., 1964. Domain variations in channel seepage flow. *J. Hydraul. Div., ASCE* 90, 55–79.

Mualem, Y., 1976. A new model for predicting the hydraulic conductivity of unsaturated porous media. *Water Resour. Res.* 12, 513–522.

Parlange, J.-Y., Hogarth, W.L., Barry, D.A., Parlange, M.B., Haverkamp, R., Ross, P.J., Steenhuis, T.S., DiCarlo, D.A., Katul, G., 1999. Analytical approximation to the solutions of Richards' equation with applications to infiltration, ponding, and time compression approximation. *Adv. Water Resour.* 23, 189–194.

Philip, J.R., 1969. Theory of infiltration. *Adv. Hydrosci.* 5 (215–296), 1969.

Phogat, V., Malik, R.S., Kumar, S., 2009. Modelling the effect of canal bed elevation on seepage and water table rise in a sand box filled with loamy soil. *Irrigat. Sci.* 27, 191–200.

Ram, S., Jaiswal, C.S., Chauhan, H.S., 1994. Transient water table rise with canal seepage and recharge. *J. Hydrol.* 163, 197–202.

Rantz, S.E., 1982. *Measurement and Computation of Streamflow*. US Geological Survey Water-Supply Paper 2175, Washington, 284 pp.

Rastogi, A.K., Prasad, B., 1992. FEM modeling to investigate seepage losses from the lined Nadiad branch canal. *J. Hydrol.* 138, 153–168.

- Salama, R.B., Otto, C.J., Fitzpatrick, R.W., 1999. Contributions of groundwater conditions to soil and water salinization. *Hydrogeol. J.* 7, 46–64.
- Schaap, M.G., Leij, F.J., van Genuchten, M.Th., 2001. Rosetta: a computer program for estimating soil hydraulic parameters with hierarchical pedotransfer functions. *J. Hydrol.* 251, 163–176.
- Shi, H.B., Tian, J.C., Liu, Q.H., 2006. *Irrigation and Drainage Engineering*. China Water Power Press, Beijing, China.
- Šimůnek, J., van Genuchten, M.Th., Šejna, M., 2008. Development and applications of the HYDRUS and STANMOD software packages, and related codes. *Vadose Zone J.* 7, 587–600.
- Sonneshein, R.S., 2001. *Methods to Quantify Seepage Beneath Levee 30*, Miami-Dade County, Florida. US Geological Survey, Water Resources Investigations Report, 01-4074.
- van Genuchten, M.Th., 1980. A closed-form equation for predicting the hydraulic conductivity of unsaturated soils. *Soil Sci. Soc. Am. J.* 44, 892–898.
- Vogel, T., Cislerova, M., 1988. On the reliability of unsaturated hydraulic conductivity calculated from the moisture retention curve. *Transp. Porous Media* 3, 1–15.
- Wachyan, E.R., Ushton, K.R., 1987. Water losses from irrigation canals. *J. Hydrol.* 92, 275–288.
- Wang, Q.J., Shao, M.A., Horton, R., 1999. Modified Green and Ampt models for layered soil infiltration and muddy water infiltration. *Soil Sci.* 164, 445–453.
- Wang, H.X., Liu, C.M., Zhang, L., 2002. Water-saving agriculture in China: an overview. *Adv. Agron.* 75.
- Wilkinson, R.W., 1986. Plastic lining on Riverton Unit, Wyoming. *J. Irrigat. Drain. Div., ASCE* 111, 287–298.